

On Pilot-Symbol-Assisted Carrier Synchronization for DVB-S2 Systems

Alan Barbieri and Giulio Colavolpe

Università di Parma, Dipartimento di Ingegneria dell'Informazione, Parma, Italy

email: barbieri@tlc.unipr.it, giulio@unipr.it

Abstract

We discuss carrier synchronization in future 2nd-generation satellite digital video broadcasting (DVB-S2) receivers. Making use of the distributed pilot symbols of the DVB-S2 standard, low-complexity techniques for fine frequency estimation and for detection in the presence of a strong phase noise, typical of consumer-grade equipments, will be described. The performance of the proposed algorithms will be analyzed through computer simulations.

I. INTRODUCTION

In future 2nd-generation satellite digital video broadcasting (DVB-S2) systems [1], carrier synchronization is a hard task. First of all, at the very low operating signal-to-noise ratio (SNR) of some of the modulation and coding (MODCOD) formats, in particular those based on the quaternary phase shift keying (QPSK) modulation and low-density parity-check (LDPC) codes with the lowest rates, frequency estimation is not sufficiently accurate and can be degraded by the occurrence of outliers. On the other hand, for those MODCODs working at high SNR values, namely those based on amplitude phase shift keying (APSK) signals and the highest code rates, the main problem is represented by the phase noise which is particularly strong, due to the use of consumer-grade equipments and possible low signaling rates. The phase noise also limits the accuracy of each frequency estimator for high SNR values [2]. Hence, it is particularly difficult to find a single low-complexity solution for carrier synchronization that could be adopted for all MODCODs and all signaling rates.

We report here the solution designed in the context of the “Study of enhanced digital transmission techniques for broadband satellite digital transmissions (BSDT),” funded by the European Space Agency. A coarse frequency synchronization is preliminarily accomplished through an automatic frequency control (AFC) loop [3]. Although this block is not necessary for the highest signaling rates, since the uncompensated frequency offset normalized to the symbol rate is low enough to guarantee that frame and timing synchronization can be successfully performed, for lower signaling rates it is practically unavoidable. From the design point of view, this coarse AFC loop does not represent a concern. In fact, a classical first-order loop, with an error signal generated according to the delay-and-multiply algorithm [4], is sufficient to guarantee the required performance. We would like to simply mention that it is necessary to adaptively compensate the amplitude distortions on the received signal, mainly due to the low-noise block and the coaxial cable at the consumer side, since they would produce a bias in the coarse frequency estimate of the AFC loop [5]. In addition, in order to avoid an increase of the already strong phase noise, due to the phase jitter of the AFC loop, the receiver can adopt the following technique. The output of the AFC loop, at the beginning of each codeword, is used to derotate the entire codeword before the further process of fine frequency estimation and compensation and detection/decoding in the presence of phase noise, that will be described in this paper. In other words, although the AFC is still running, we use its output frozen at the beginning of each codeword. In this way, each codeword is not only affected by a constant frequency error equal to the instantaneous frequency error of the AFC loop at the beginning of the codeword, but also by the entire Doppler rate (and also by the received phase noise). However, it can be shown that the amount of this Doppler rate does not affect the performance of the algorithm we propose for joint detection and decoding in the presence of phase noise.

The fine frequency estimation and compensation and the problem of detection and decoding in the presence of phase noise deserve a greater attention and in this paper we will focus on them. In particular, after the description in Section II of the system model, in Section III we will consider the frequency estimation of the residual frequency offset after the coarse AFC loop. This residual frequency offset will be assumed constant over a frame and, due to the coherence time of the AFC loop, independent frame by frame. The low-complexity technique that will be described makes use of distributed pilot symbols, as in the DVB-S2 standard, and the presence of the decoder. The more challenging problem, that is the detection and decoding in the presence of phase noise, will be faced in Section IV. Finally, in Section V the performance of the described algorithms will be discussed, whereas in Section VI some conclusions will be drawn.

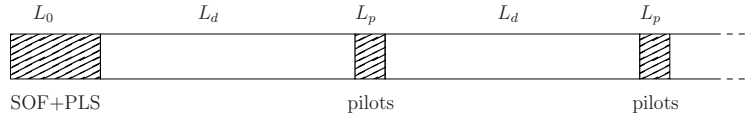


Fig. 1. Pictorial representation of a DVB-S2 frame.

II. SYSTEM MODEL

We consider the transmission of a sequence of K complex modulation symbols $\mathbf{c} = (c_0, c_1, \dots, c_{K-1})$ over an additive white Gaussian noise (AWGN) channel affected by an uncompensated frequency error ν and a time-varying phase θ_k . Symbols c_k are linearly modulated. Assuming Nyquist transmitted pulses, matched filtering, and phase variations slow enough so as no intersymbol interference arises, the discrete-time baseband complex equivalent channel model at the receiver is given by

$$r_k = Ac_k e^{j(2\pi\nu kT + \theta_k)} + w_k, \quad k = 0, \dots, K-1, \quad (1)$$

being A an unknown gain, T the symbol duration, and $\{w_k\}$ the additive noise samples, assumed independent and identically distributed, complex, circularly symmetric Gaussian random variables, each with mean zero and variance equal to $2\sigma^2$. We assume that the sequence \mathbf{c} is a codeword of the channel code \mathcal{C} constructed over an M -ary modulation constellation $\mathcal{X} \subset \mathbb{C}$. We include the preamble and the pilot symbols (known to the receiver) as a part of the code \mathcal{C} . In Fig. 1, a pictorial representation of the DVB-S2 frame format is reported. At the beginning of each frame $L_0 = 90$ known symbols, representing the start-of-frame (SOF) and the physical layer signaling (PLS) code, are inserted. Then, P pilot fields, of $L_p = 36$ symbols each, are inserted every $L_d = 1440$ coded symbols. The number P of pilot fields depends on the employed modulation (for example, $P = 22$ for QPSK, while $P = 8$ for 32-APSK).

The vector of channel phases $\boldsymbol{\theta} = (\theta_0, \theta_1, \dots, \theta_{K-1})$ is random, unknown to both transmitter and receiver, and statistically independent of \mathbf{c} , $\{w_k\}$, ν , and A . The estimation of the gain A is not considered here since discussed in [6]. Hence, without loss of generality, in the following we assume $A = 1$. As already mentioned, we assume that the residual frequency offset ν after the coarse AFC is constant over a frame and independent frame by frame.

III. FINE FREQUENCY ESTIMATION

The aim of the fine frequency estimation block is to reduce the residual offset ν in (1) to a value tolerable by the detection algorithm. In order to find this target value, it is necessary to anticipate some concepts related to the detection algorithm that will be described in Section IV. It is a data-aided/soft-decision-directed (DA/sDD) soft-input soft-output (SISO) algorithm which, at the first iteration, exploits the pilot symbols only. Let us consider Fig. 2, representing a part of a typical transmitted frame between two consecutive pilot fields. Phase variations between the two consecutive fields are mainly induced by the residual frequency offset ν and, secondarily, by the phase noise. Clearly, two values of the residual normalized frequency offset which differ by a multiple of $1/(L_d + L_p)$ cannot be distinguished by the detection algorithm, since they induce the same phase on each pilot field. However, they induce a completely different phase variation on data symbols between the pilot fields. Therefore, it should be clear that it is required to have a

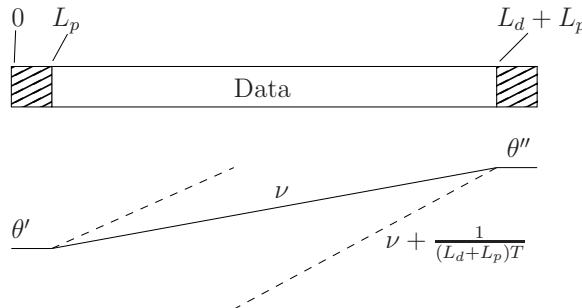


Fig. 2. Pictorial representation of a *cycle slip* event.

residual normalized frequency error, after the fine frequency estimation and compensation block, within the range¹ $\pm 1/2(L_d + L_p)$. If this is not the case, the phase estimates on data symbols between two pilot fields are completely wrong and the frame cannot be decoded, resulting in a high number of bit errors. This event was already described in [7], where the authors called it *cycle slip*, although it should not be confused with the cycle slip in a phase-locked loop.

Hence, the aim of the fine frequency estimation algorithm is to reduce the frequency offset such that $P\{|\nu| > \frac{1}{2(L_d + L_p)T}\} < FER_{\text{target}}$, where FER_{target} is the target frame-error rate (FER). Indeed, if ν is inside the required range, it will be perfectly compensated by the detection algorithm. Under the hypothesis of a zero-mean Gaussian-distributed residual frequency error after the fine frequency estimation and compensation block, the above mentioned requirement is equivalent to require a root mean square error (RMSE) less than about 1/6 of the maximum tolerable value. As a final remark, we would like to point out that a more sparse pilot distribution would have led to less stringent constraints on the residual frequency offset, thus leading to lower complexity estimation algorithms. On the other hand, in the absence of pilot symbols the maximum tolerable frequency offset decreases dramatically. Hence an estimation algorithm characterized by an extremely small RMSE should be employed in this situation.

Data-Aided and Code-Aided Estimation Algorithm

We propose here a solution to the problem of the fine frequency estimation, with a good robustness and a low computational complexity, which takes advantage of the distributed pilot symbols and of the presence of the decoder, and whose only disadvantage is a slight increase of the decoding latency. It is based on a three-step procedure:

Coarse DA step. A DA estimate $\hat{\nu}_1$ is first computed on the preamble, for example by using the Mengali and Morelli (MM) algorithm [4], [8].

Fine DA step. A new DA estimate $\hat{\nu}_2$ is derived, based on the distributed pilot symbols, by means of a reduced-complexity MM algorithm:²

$$\hat{\nu}_2 = \frac{1}{2\pi(L_d + L_p)T} \arg \left[\sum_{p=1}^{P-1} \sum_{k=0}^{L_p-1} z_{L_0 + L_d + p(L_d + L_p) + k} z_{L_0 + L_d + (p-1)(L_d + L_p) + k}^* \right] \quad (2)$$

where $z_n = r_n c_n^* e^{-j2\pi\hat{\nu}_1 nT}$. It is worth noticing that the estimator in (2) exhibits a very low RMSE, since exploits the large distance between the pilot symbols, but also an estimation range limited in $\pm \frac{1}{2(L_d + L_p)T}$. Therefore, in practice a set of estimates of the form $\hat{\nu}_1 + \hat{\nu}_2 + \frac{\ell}{(L_d + L_p)T}$, $\ell = 0, \pm 1, \pm 2, \dots$, are obtained. Depending on the accuracy of the first estimation step (namely, the coarse DA), the number of valid estimates which cannot be distinguished changes, although in practice five estimates are often sufficient. Hence, a selection step is required.

Selection. A code-aided selection algorithm is carried out to choose one among the several estimates obtained in the previous steps. The employed selection algorithm is based upon a simple consideration: when the iterative joint detection and decoding algorithm described in Section IV starts with the correct frequency, the bit errors, as well as the code syndrome, fall down very quickly, provided that the SNR is above the convergence threshold. On the contrary, with the wrong frequency, the bit errors and the code syndrome remain stuck at very high values. Therefore, a straightforward way to know if the trial frequency offset value is correct or wrong, is to check the code syndrome (which is always done in the LDPC decoding) after one decoding iteration.

As a final remark, we would like to point out that in order to further decrease the probability of the event “choice of a wrong frequency estimate”, we can perform more than one iteration for each candidate frequency estimate. In fact, for the correct frequency value, under the hypothesis of convergence of the iterative detection and decoding algorithm, the syndrome value goes down to zero with the iterations, whereas for a wrong frequency it remains stuck at a very large value.

IV. THE CBC ALGORITHM

In [9], based on the framework of factor graphs (FGs) and the sum-product algorithm (SPA), a new efficient algorithm for iterative detection and decoding of channel codes transmitted over channels affected by phase noise has been derived. The approach is Bayesian, i.e., the unknown channel parameter is modeled as a stochastic process with known statistics. In particular, the phase noise is assumed modeled as a Wiener process, with incremental variance over a signaling

¹For the standard DVB-S2 pilot symbols distribution, since $L_d = 1440$ and $L_p = 36$, the range becomes $\pm 3.38 \cdot 10^{-4}$.

²It can be easily verified that it is the MM algorithm using one autocorrelation term only.

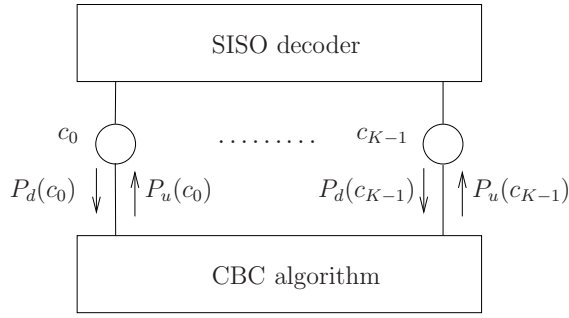


Fig. 3. Pictorial representation of the iterative receiver.

interval equal to σ_{Δ}^2 . The FG corresponding to the joint a posteriori probability distribution of the information message bits given the received signal is built and the SPA is used to compute the posterior marginal distributions. Bit-by-bit decisions are then made, based on the resulting posterior marginals. The FG includes the knowledge of the unknown parameter statistics. Expectation over the unknown parameters is implicitly performed by the SPA as part of the marginalization.

We now briefly review the derivation of the algorithm proposed in [9] (denoted to as the “CBC” algorithm in the following). Let us focus on the above mentioned Wiener phase noise. While the SPA is well-suited to handle discrete random variables, characterized by a probability mass function (pmf), the channel parameters are, in this case, continuous random variables, characterized by a pdf. The SPA for continuous random variables involves integration and computation of continuous pdfs, and it is not suited for direct implementation. A solution for this problem is suggested in [10] and consists of the use of *canonical distributions*, i.e., the pdfs computed by the SPA are constrained to be in a certain “canonical” family, characterized by some parameterization. Hence, the SPA has just to forward the parameters of the pdf rather than the pdf itself. Clearly, several different algorithms can be obtained depending of the choice of the canonical distribution.

In [9], an approach based on a Tikhonov parameterization has been proposed. It yields a one-dimensional forward-backward recursion that can be regarded (roughly speaking) as a non-linear version of the Kalman smoother. Remarkably, its performance is nearly as good as the discretized-phase approach (nearly optimal) with considerable lower complexity [9].³

Let us consider the Fig. 3, which represents a pictorial description of the iterative receiver. Two blocks, namely the SISO decoder (e.g., the LDPC decoder in the DVB-S2 scenario) and the CBC algorithm are iteratively activated and exchange themselves the extrinsic probabilities of the coded symbols. We denote by $P_d(c_k)$ the a priori probability of the modulation symbol c_k at time epoch k provided by the decoder and by $P_u(c_k)$ the extrinsic a posteriori probability evaluated by the CBC algorithm. These probabilities are iteratively updated, but the explicit reference on the iteration number is dropped for simplicity.

The CBC algorithm is based on the following steps:

- 1) Given the messages $P_d(c_k)$, $k = 0, 1, \dots, K - 1$, $c_k \in \mathcal{X}$, provided by the decoder, for $k = 0, 1, \dots, K - 1$, compute

$$\alpha_k = \sum_{c_k} P_d(c_k) c_k \quad (3)$$

and

$$\beta_k = \sum_{c_k} P_d(c_k) |c_k|^2. \quad (4)$$

The complex parameter α_k and the real one β_k are respectively the first and second order moments of the a priori pmf $P_d(c_k)$.

³In [9], it is shown that a minimum number of pilot symbols is necessary for this algorithm to bootstrap the iterative decoder in the case of strong phase noise and long codewords.

- 2) Forward recursion. It consists of the evaluation of a sequence of complex parameters, one for each time epoch, denoted to as $a_{f,k}$ and implicitly representing an estimate of the channel phase at time k . Let $a_{f,0} = 0$. For all $k = 1, 2, \dots, K - 1$, compute

$$a'_{f,k} = a_{f,k-1} + 2 \frac{r_{k-1} \alpha_{k-1}^*}{2\sigma^2 + \beta_{k-1} - |\alpha_{k-1}|^2} \quad (5)$$

and then

$$a_{f,k} = \frac{a'_{f,k}}{1 + \sigma_{\Delta}^2 |a'_{f,k}|}. \quad (6)$$

In the previous recursive equation, σ_{Δ} is, as already mentioned, the standard deviation of the increment of the Wiener process. In the numerical results, we will consider a phase noise that cannot be modeled as a Wiener process. In that case, σ_{Δ} must be considered as a design parameter to be optimized by computer simulation for the phase noise at hand.

- 3) Backward recursion. Similarly to the forward recursion, a sequence of complex parameters $a_{b,k}$ is recursively updated during this stage. Let $a_{b,K-1} = 0$. For all $k = K - 2, \dots, 1, 0$, compute

$$a'_{b,k} = a_{b,k+1} + 2 \frac{r_{k+1} \alpha_{k+1}^*}{2\sigma^2 + \beta_{k+1} - |\alpha_{k+1}|^2} \quad (7)$$

and then

$$a_{b,k} = \frac{a'_{b,k}}{1 + \sigma_{\Delta}^2 |a'_{b,k}|}. \quad (8)$$

- 4) The messages sent to the decoder for a new iteration will be, for all $k = 0, 1, \dots, K - 1$

$$P_u(c_k) \propto \exp \left\{ -\frac{|c_k|^2}{2\sigma^2} \right\} I_0 \left(\left| a_{f,k} + a_{b,k} + \frac{r_k c_k^*}{\sigma^2} \right| \right) \quad (9)$$

$$\simeq \exp \left\{ -\frac{|c_k|^2}{2\sigma^2} + \left| a_{f,k} + a_{b,k} + \frac{r_k c_k^*}{\sigma^2} \right| \right\}. \quad (10)$$

where $I_0(\cdot)$ is the modified Bessel function of the first kind of order zero. Eq. (10) stems from the fact that, for a large enough argument, $I_0(x) \simeq e^x$.

Hence, the algorithm is based on a forward-backward schedule performed over the whole codeword. Alternatively, a mixed serial-parallel schedule, performing separate and parallel forward-backward recursions between pilot fields, can be adopted with a negligible performance loss. In this way, the degree of parallelism of the implementation can be increased.

V. NUMERICAL RESULTS

In this Section, the performance of the proposed estimation and detection algorithms is assessed by computer simulations. Where not explicitly stated, the phase noise we consider is the DVB-S2 compliant ESA phase noise model for consumer-grade equipments at a baud rate of 10 Mbaud [7], [11].

Performance of the frequency estimation algorithm

In order to evaluate the performance of the proposed frequency estimation algorithm, three kinds of computer simulations are employed. In the first one, we evaluate the outlier probability of the first step of the algorithm, that is the coarse DA estimation, versus E_S/N_0 , E_S being the received signal energy per modulation symbol and N_0 the one-sided noise power spectral density. In this case, the outlier probability is defined in the following way: let us assume that we want to keep and test through the decoder a maximum of $2n + 1$ estimates after the fine DA step. Hence, the algorithm works only if the estimation error of the first step lies inside an interval of width $\frac{2n+1}{L_d+L_p}$ centered around zero. On the contrary, when the true frequency offset value does not belong to the set of estimates produced by the first two steps, the frame will be decoded incorrectly. Thus, in order to carry out correct decoding, the outlier probability must be lower than the target FER. In Fig. 4, the outlier probability for different values of the maximum number of employed estimates is shown. As it can be seen, depending on the working SNR, a different number of estimates has to be kept and fed to the selection step. For example, for higher-order modulation formats, characterized by a large working SNR, 3 trial values are sufficient whereas, in all other cases, we need that the coarse + fine DA steps produce 5 estimates. The same figure also tells that with the standardized pilot distribution a classical DA frequency estimation strategy, producing only one estimate, fails.

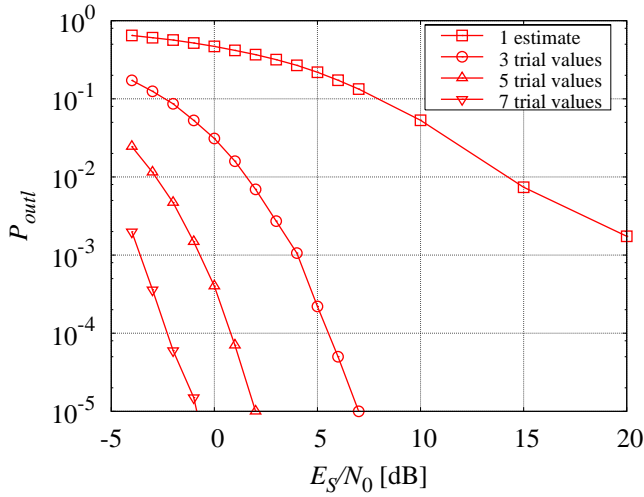


Fig. 4. Outlier probability of the coarse DA step, for different values of the number of estimated values fed to the selection step.

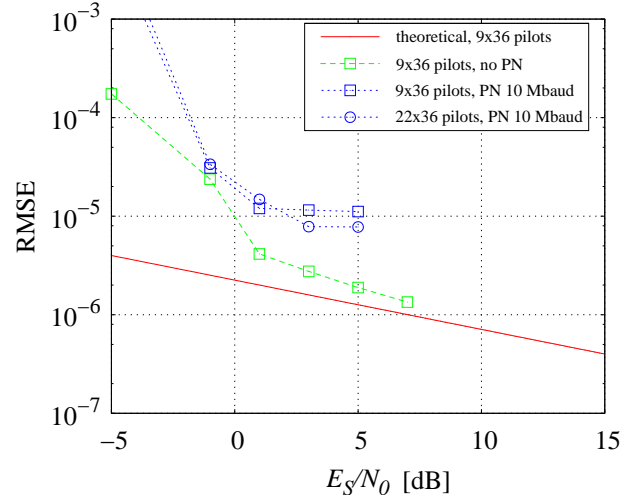


Fig. 5. Performance of the code-aided DA estimation algorithm in case of selection of the correct frequency estimate.

In the second computer simulation we evaluate the estimation accuracy of the first two steps under the hypothesis of genie-selection, by taking into account a total of five estimated values. In other words, we consider the estimate $\hat{\nu}_1 + \hat{\nu}_2 + \frac{\hat{\ell}}{(L_d + L_p)T}$ being $\hat{\ell}$ (which can take on the values $0, \pm 1, \pm 2$) the integer ensuring the lowest error. Fig. 5 refers to the estimation accuracy of the proposed algorithm, under the hypothesis of correct selection. As it can be seen, in the absence of phase noise the estimation accuracy lean on the following theoretical RMSE curve, valid for large SNR:

$$RMSE_{theor} = \sqrt{\frac{2P - 3}{2\pi^2 L_p (L_d + L_p)^2 (P - 1)^2 \frac{E_s}{N_0} T^2}}. \quad (11)$$

Eq. (11) was obtained by substituting $z_k = r_k c_k^*$ in (2), neglecting the noise by noise terms and replacing $\arg(1 + u)$ with $\text{Im}(u)$, which is a valid approximation for small u . On the other hand, it is known that, in the presence of phase noise, a floor in the RMSE of the frequency estimator appears, regardless of the employed estimation algorithm, namely it is not possible to reduce the RMSE below a given threshold by simply increasing the SNR [2]. When only five estimates are employed, the target accuracy that let the algorithm for joint detection and decoding described in Section IV work, is reached for $E_S/N_0 \geq 1$ dB.

Finally, in the last computer simulation, we evaluate the probability that the code-aided selection algorithm chooses the wrong estimate. Clearly, when this event occurs the LDPC decoder produces a very large number of bit errors. Hence, we must ensure that the probability of this event is sufficiently lower than the target FER. In Fig. 6(a), the histogram of the code syndrome for the 8-PSK modulation, with the low-density parity-check (LDPC) of rate $r = 2/3$ at $E_b/N_0 = 3.5$ dB, is shown. The leftmost histogram was obtained by considering a residual normalized frequency error with a Gaussian distribution having zero mean and a standard deviation $3 \cdot 10^{-5}$, independently generated frame by frame, while the rightmost histogram refers to wrong frequency values (namely, with absolute errors larger than $\frac{1}{2(L_d + L_p)}$). The detection is performed by means of the CBC algorithm described in Section IV. Only one iteration of the detector and decoder is allowed. As it can be seen, there is a huge separation between the histograms. Hence the proposed technique is viable for the considered scenario: after one iteration of detector and decoder, if the code syndrome is below a threshold of 7000, we can say that we have found the right frequency estimate. Otherwise, we go ahead to the next value. Clearly, this separation increases for larger SNR values.

Since, in a code-aided technique, the most critical case occurs for the less robust code, in Fig. 6(b) we consider the LDPC code with $r = 9/10$, along with the two farthest modulations: QPSK and 32-APSK at $E_b/N_0 = 4.0$ dB and $E_b/N_0 = 9.0$ dB, respectively, E_b being the received signal energy per information bit. In the case of wrong frequencies, the syndrome histograms for the two different modulations are more or less overlapped. On the contrary, the separation between the histograms for correct and wrong frequency estimates are completely different for the two modulations. The most critical case occurs for 32-APSK, due to its lower robustness to phase errors, but still in this case there is a separation high enough to ensure that, by using a syndrome threshold value of about 2150, the event

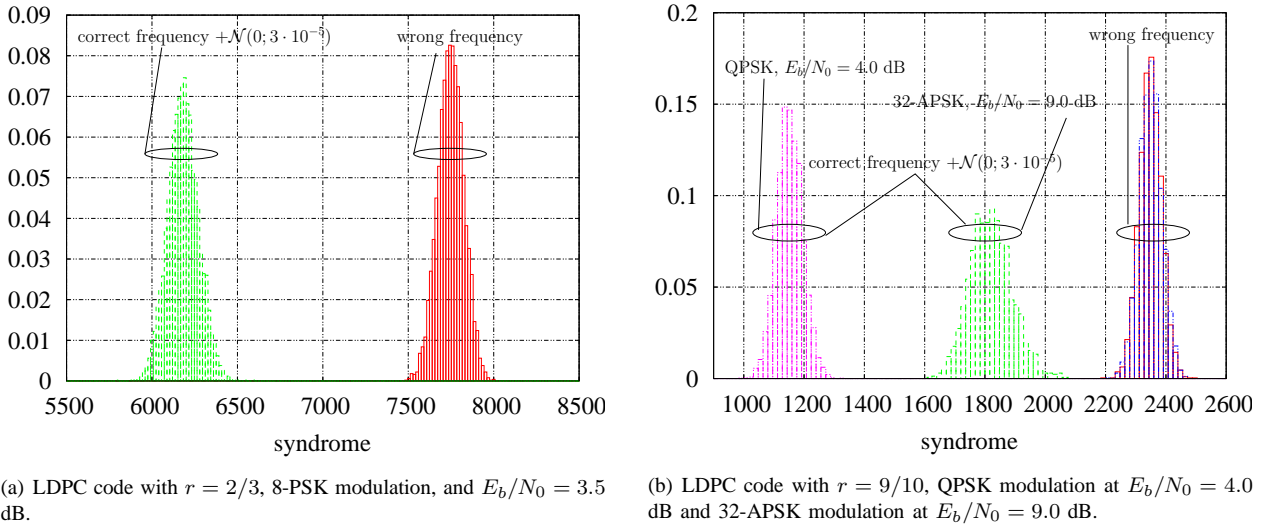


Fig. 6. Syndrome histogram at the end of the first iteration.

“choice of a wrong frequency estimate” has a negligible probability.

Performance of the CBC algorithm

The performance of the proposed detection algorithm is assessed by computer simulations in terms of bit error rate (BER) versus E_b/N_0 . A maximum of 50 iterations of the iterative receiver is allowed. For each simulated point, a minimum of 50 frame errors is counted.

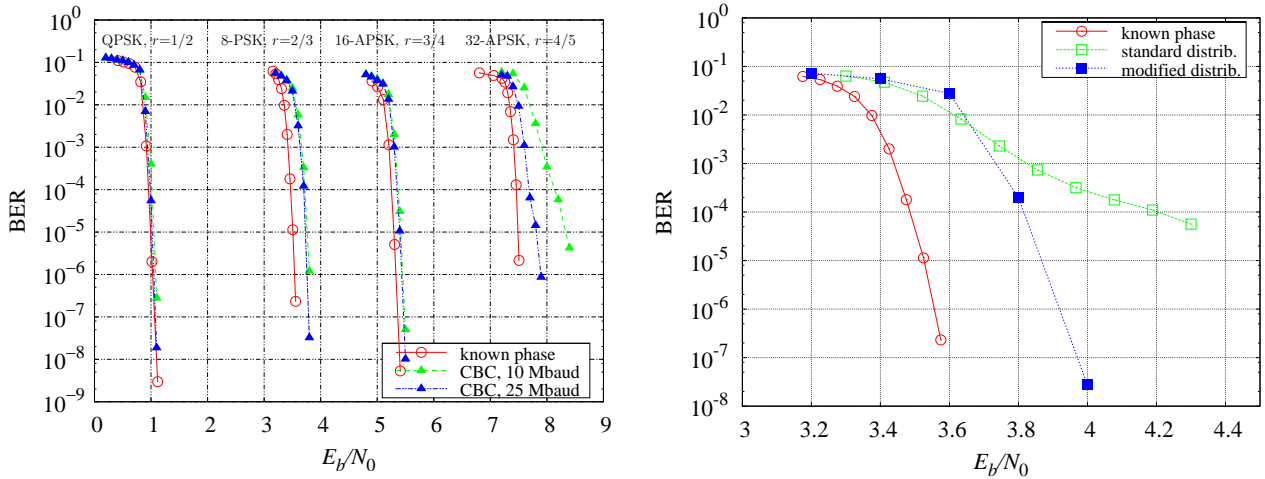
In all simulated cases, pilot symbols, following the standardized distribution, are inserted in the transmitted codeword in order to make the iterative decoding algorithm bootstrap. Pilot symbols involve a slight decrease of the effective information rate, resulting in an increase in the required signal-to-noise ratio. This increase has been introduced artificially in the curve labeled “known phase” for the sake of comparison. Hence, the gap between the “known phase” curve and the others is not related to the rate decrease due to pilot symbols.

Despite the CBC algorithm was developed with a Wiener phase noise model in mind [9], in the computer simulations we consider the DVB-S2 compliant ESA phase noise model. In Fig. 7(a), we consider four standardized LDPC codes with codewords of length 64800 [1], namely a rate-1/2 code mapped onto a QPSK modulation, a rate-2/3 code mapped onto an 8-PSK modulation, a rate-3/4 code mapped onto a 16-APSK modulation and a rate-4/5 code mapped onto a 32-APSK modulation. The above mentioned phase noise ESA model is considered, for a baud rate of 10 Mbaud or 25 Mbaud. The CBC algorithm exhibits only a minor loss due to phase noise, less than 0.1 dB for QPSK, 8-PSK and 16-APSK modulations. On the contrary, the loss for 32-APSK is larger, due to the larger sensitivity of this constellation to phase mismatches as well as to the higher code rate. Moreover, as it can be seen, the loss is larger for lower signaling rates, since the lowest the signaling rate the fastest the phase noise.

In Fig. 7(b), we consider the rate-2/3 code mapped onto an 8-PSK, but the DVB-S2 compliant phase noise for a baud rate of 1 Mbaud is employed. Two pilot symbols distributions are taken into account. “Standard” refers to the standardized distribution (i.e., 36 pilot symbols every 1476 transmitted symbols [1]) while “modified” refers to a more sparse distribution characterized by 3 pilot symbols every 123 transmitted symbols. It is worth noticing that, despite the insertion rate is the same for the two cases, the performance of the CBC algorithm for the modified distribution is much better. The bad performance of the CBC algorithm for the standard distribution in the considered scenario is due to the fact that the phase noise corresponding to 1 Mbaud varies faster than that corresponding to 10 Mbaud, thus leads to a non-negligible loss if the pilot fields are too far one of each other, as in the standard pilot distribution.

VI. CONCLUSIONS

We discussed pilot-symbol-assisted carrier synchronization in future DVB-S2 receivers. A single low-complexity and robust solution has been identified and its performance analyzed. In the absence of pilots, however, this solution cannot be employed, since the fine frequency estimator heavily exploits pilots and in addition, the sensitivity of the CBC algorithm to frequency errors highly increases in the absence of pilots.



(a) QPSK, 8-PSK, 16-APSK, and 32-APSK modulations, with standard pilot distribution

(b) LDPC code with $r = 2/3$ mapped onto the 8-PSK modulation at a baud rate of 1 Mbaud

Fig. 7. Performance of the proposed algorithm based on Tikhonov parameterization. The ESA phase model for several baud rates is considered.

We would like to remark that a more sparse pilot distribution would have been beneficial to reduce the receiver complexity and improve its performance. In fact, from a computational complexity point of view the frequency estimation algorithm would have been simplified since the selection step could have been avoided. From a performance point of view, the detection algorithm would have been able to cope with the strongest phase noise, namely that for the lowest signaling rate.

ACKNOWLEDGMENTS

This work is part of the “Study of enhanced digital transmission techniques for broadband satellite digital transmissions (BSDT)” funded by the European Space Agency, ESA-ESTEC, Noordwijk, The Netherlands, under contract no. 19370.

REFERENCES

- [1] ETSI, “ETSI - DVB-S2 74r13, Digital Video Broadcasting (DVB): Second generation framing structure, channel coding and modulation systems for Broadcasting, Interactive Services, News Gathering and other broadband satellite applications,” 2003.
- [2] A. Barbieri, D. Bolletta, and G. Colavolpe, “On the Cramer-Rao bound for carrier frequency estimation in the presence of phase noise,” in *Proc. IEEE Global Telecommun. Conf.*, (St. Louis, MO, U.S.A.), pp. 720–724, 2005.
- [3] A. Barbieri, A. Cero, D. Fertonani, and G. Colavolpe, “BSDT — Technical note TN01: Modem algorithms design specification for the broadband forward link with linear modulations — Part 1: Carrier synchronization,” tech. rep., July 2006. ESA Contract No. 19370.
- [4] U. Mengali and A. N. D’Andrea, *Synchronization Techniques for Digital Receivers (Applications of Communications Theory)*. Plenum Press, 1997.
- [5] D. Fertonani, A. Barbieri, G. Colavolpe, and D. Delaruelle, “Estimation and compensation of linear amplitude distortions,” in *9-th Intern. Work. on Signal Processing for Space Commun.*, (ESTEC, Noordwijk, The Netherlands), Sept. 2006.
- [6] A. Barbieri, A. Cero, and G. Colavolpe, “Iterative per-frame gain and SNR estimation for DVB-S2 receivers,” in *9-th Intern. Work. on Signal Processing for Space Commun.*, (ESTEC, Noordwijk, The Netherlands), Sept. 2006.
- [7] A. Ginesi, D. Fittipaldi, A. Bigi, and R. De Gaudenzi, “Pilot-aided carrier synchronization techniques for broadband satellite transmissions,” tech. rep., ESA-ESTEC, Sept. 2003.
- [8] U. Mengali and M. Morelli, “Data-aided frequency estimation for burst digital transmission,” *IEEE Trans. Commun.*, vol. 45, pp. 23–25, Jan. 1997.
- [9] G. Colavolpe, A. Barbieri, and G. Caire, “Algorithms for iterative decoding in the presence of strong phase noise,” *IEEE J. Select. Areas Commun.*, vol. 23, pp. 1748–1757, Sept. 2005.
- [10] A. P. Worthen and W. E. Stark, “Unified design of iterative receivers using factor graphs,” *IEEE Trans. Inform. Theory*, vol. 47, pp. 843–849, Feb. 2001.
- [11] L. Benvenuti, L. Giugno, V. Lottici, and M. Luise, “Code-aware carrier phase noise compensation on turbo-coded spectrally-efficient high-order modulations,” in *8-th Intern. Work. on Signal Processing for Space Commun.*, (Catania, Italy), pp. 177–184, Sept. 2003.